

Chronological operation simulation framework for regional power system under high penetration of renewable energy using meteorological data



Shiwu Liao, Wei Yao*, Xingning Han, Jinyu Wen, Shijie Cheng

State Key Laboratory of Advanced Electromagnetic Engineering and Technology, School of Electrical and Electronic Engineering, Huazhong University of Science and Technology, Wuhan 430074, China

HIGHLIGHTS

- A three-step chronological operation simulation framework (COSF) is proposed.
- The COSF generates wind and solar output profiles with meteorological data.
- Time-domain partitioning and a roll-back mechanism are used to improve the efficiency of COSF.
- Simulation results verify the accuracy and computation efficiency of the COSF.

ARTICLE INFO

Article history:

Received 8 January 2017

Received in revised form 24 June 2017

Accepted 28 June 2017

Keywords:

Chronological operation simulation
Power system operation
Meteorological data
Unit commitment
Simulation framework

ABSTRACT

Chronological operation simulation (COS) is an essential tool for planning and analyzing power systems under high penetration of renewable energy. Conventional COS methods heavily depend on the availability of renewable power output data to obtain accurate results, and often require hours or even days of computational time while the sequential simulation could easily get infeasible for power systems with intensive flexibility. To cover the absence of output data for newly proposed wind and solar projects and accelerate the computation speed, this paper proposes a novel COS simulation framework for regional power systems with high penetration of renewable energies using meteorological data. The proposed simulation framework consists of the following three steps: data preparation, modeling and solving, and result output. In the data preparation step, wind, solar power output profiles and heat demands are converted from public accessible meteorological data. Then in the modeling and solving step, a unit commitment based COS model for simulating the hourly operation of power and heat sectors is proposed, and the proposed model is solved with a time domain partitioning (TDP) and a rollback mechanism to accelerate the computation speed as well as avoiding infeasible solutions. The accuracy of the wind and solar power output converted from meteorological data is verified through comparing with measured power output. Moreover, the feasibility and accuracy of utilizing the proposed COS framework to simulate the operation of a real regional power system is also verified through the 2015 annual operation statistics of the Northwest China Grid.

© 2017 Elsevier Ltd. All rights reserved.

1. Introduction

As a major solution to curb the CO₂ emission, renewable energy is developing rapidly all over the world. In 2015, 63 GW wind and 50 GW solar were installed over the globe [1–3], which was unprecedented for the wind and solar industry. To achieve the

target set in the COP21 of keeping global warming less than 2 °C above the preindustrial level [4], renewable energies such as the wind and solar will continue to grow rapidly. Therefore, evaluating the potential of renewable energy has become a key area of interest within energy planning and policy making. A crucial element in the development of renewable energy is often to show coherent technical analyses of how renewable energy can be implemented, and how the renewable energy affects other parts of the energy system. Such analyses require simulation methods that can give answers to these issues by modeling the operation of the energy systems [5,6].

* Corresponding author.

E-mail addresses: liaoshiwu@gmail.com (S. Liao), w.yao@hust.edu.cn (W. Yao), xingning.han@gmail.com (X. Han), jinyu.wen@hust.edu.cn (J. Wen), sjcheng@hust.edu.cn (S. Cheng).

Incorporating large amounts of intrinsically variable renewable power will heavily affect the chronological operation of power systems. On the other hand, the intra-interval characteristics of power system operation will also restrict the integration of renewable energy. Therefore, among all methods developed for analyzing the renewable energy integration in energy systems, chronological operation simulation (COS) is an essential tool because it could simulate the chronological interactions between the renewable generations and the power system [7]. The COS simulates the operation of energy systems by finding the least-cost solution of generating sufficient energy to meet demand in a sequential way, namely year around operations are simulated by consecutively running short-term simulations (e.g. daily or weekly simulations) to find the optimal solution for each time interval given the solution of the previous time interval. The solution is constrained by transmission limits, generator operation characteristics (e.g., startup costs, ramp rates, and maintenance outages), and reserve requirements to meet intra-interval generation-demand imbalances. Typically, COS is used to simulate operations on an annual horizon to capture the seasonal variability of load and renewable resource. As illustrated in Fig. 1, COS is widely adopted by all participants of the power system construction, operation and administration. With the growing penetration of renewable energy in power systems, it is essential to have an accurate and reliable COS framework to quantify the generation potential and grid-accommodation potential of proposed renewable projects or pledged renewable targets. Currently, computer tools like BALMOREL and EnergyPLAN are widely adopted to carry out the COS [8–10], and plenty of researches about the renewable integration are performed based on the COS [11–15]. Although these tools and researches provide a feasible way of adopting COS to analyze the renewable integration in power systems, current COS methods still have two bottlenecks constraining their applications in analyzing planned renewable projects or evaluating future energy targets, and in simulating large-scale power systems with very intensive flexibilities.

For the COS, renewable power output profiles are required [16,17]. However, for newly proposed projects or future renewable targets, no historical renewable power output data are available. Moreover, the historical wind and solar power outputs with high temporal resolution are not made public at most places in the world. Hence, how to obtain wind and solar power output from alternative data sources is important for COS of regional power system integrated high penetration renewable energy.

Besides the heavy dependence on renewable output data, the computation efficiency is also a bottleneck for the COS. Owing to the large number of generators in regional grids, the computation of a sequential COS still could take several hours or even a few days

[18,19]. In addition, caused by the intensive flexibility of power systems with renewable energy deeply penetrated, the sequential simulation could easily get infeasible solutions at any time interval during the annual simulation [20,21], then there will be no complete COS results available for applications.

To address the bottlenecks of renewable output profile dependence and computation efficiency in the COS, this paper proposes a simulation framework that obtains wind and solar output from public accessible meteorological data and simulates the annual operation of regional power systems fast and reliably. The proposed framework consists of three steps: data preparation, modeling and solving, and result output. In the data preparation step, a public accessible meteorological database, which provides hourly wind speed, surface irradiance, and surface temperature data, is adopted to obtain the hourly wind, solar power output, and the heat load for combined heat and power (CHP) units. After all input data are prepared, the modeling and solving step proposes a COS model for simulating the hourly operation of combined power and heat sectors, and adopts a time domain partitioning (TDP) method and a rollback mechanism to simulate the year around operation. With the proposed COS model and solving strategy, the computation speed is significantly accelerated and infeasible results can be avoided. After the modeling and solving step gets finished, results from all parallel processes are combined in the result output step. The accuracy of wind and solar output profiles converted from meteorological data is verified through comparing with the measured output from practical wind and solar projects. And the COS result of Northwest China Grid in 2015 obtained from the proposed framework is verified in good consistency with the statistical data released by China National Energy Administration (NEA) [22,23] and the State Grid Corporation of China [24]. Compared with existing studies, the main contributions of this paper are four folds:

- A novel COS framework for analyzing the integration of renewable energies into power and heat systems is proposed. Compared with the existing COS tools, the proposed framework can analyze newly proposed renewable projects and future energy targets accurately, and can avoid infeasibility and reduce the computation time for analyzing large-scale power systems with very intensive flexibilities. Moreover, the proposed framework can be used to investigate the potential renewable curtailments in the future and to aid the selection of techniques for reducing the curtailments.
- A method that can obtain wind, solar power output and heat load for CHP units from public accessible meteorological and geographical database is proposed, which makes the proposed

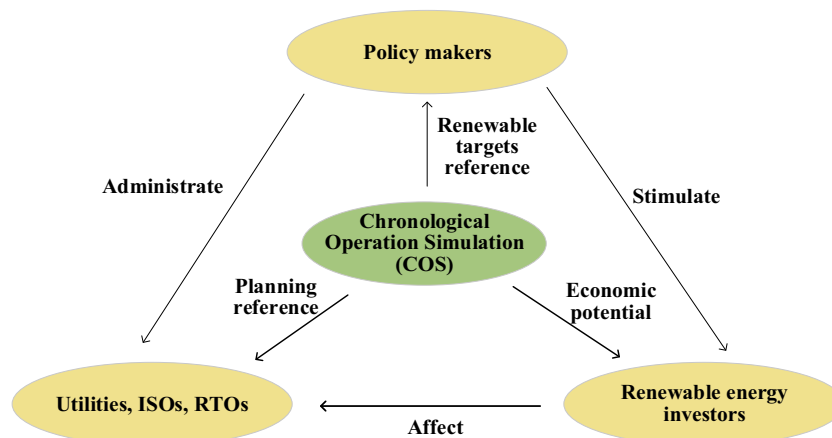


Fig. 1. Applications of COS in power system.

framework be capable of simulating the operation of power systems with proposed renewable projects or future renewable targets.

- A COS model is proposed to simulate the hourly operation of combined power and heat sectors, in which the power system is partitioned into subsystems to decrease the model complexity and improve the computational efficiency. Moreover, a solving acceleration strategy consisting of a rollback mechanism and a time domain partitioning (TDP) method is proposed to accelerate the computation speed and guarantee feasible results.
- The feasibility and accuracy of the proposed COS framework adopted to simulate the operation of a practical power system are verified by comparing the simulation results of Northwest China Grid in 2015 with official statistics. The comparison results reveal that the difference between the simulation results obtained from the proposed framework and the practical operation statistics is less than 6.8%.

The rest of this paper is organized as follows. In Section 2, the structure of the proposed COS framework for the regional power system is introduced. To demonstrate the proposed COS framework in detail, the data preparation step and modeling and solving step are elaborated in s 3 and 4, respectively. The process of adopting the proposed framework to simulate the operation of Northwest China Grid (NWCG) in 2015 and verification of the simulation results are presented in Section 5. Conclusions are drawn in Section 6.

2. Structure of the proposed simulation framework

To relieve the conventional COSs from heavily depending on historical wind and solar output data and to accelerate simulation speed, this paper proposes a framework for COS consisting of three steps: data preparation, modeling and solving, and result output. The structure of the proposed simulation framework is illustrated in Fig. 2. The three steps are introduced in detail as follows:

- *Step I: Data Preparation.* In this step, wind and solar output profiles, heat load for CHP units, parameters of conventional generators, load forecasts and inter-regional transmission data are prepared for the next step. Among all data prepared in this step, wind, solar power output and heat load are converted from public accessible meteorological data, population distribution data and administration area data. The power system is partitioned into sub-systems at critical tie-lines.
- *Step II: Modeling and Solving.* Based on the data prepared in Step I, a COS model for simulating the operation of combined power and heat sectors is formulated. Then a rollback mechanism is proposed to avoid infeasible results during simulating the operation of all months in parallel.
- *Step III: Result Output.* In this step, monthly simulation results are combined as annual simulation results, so that hourly and annual total wind & solar accommodation results, the operation of conventional generations, fuel consumption and flexibility adequacy can be outputted for different analyzing purposes.

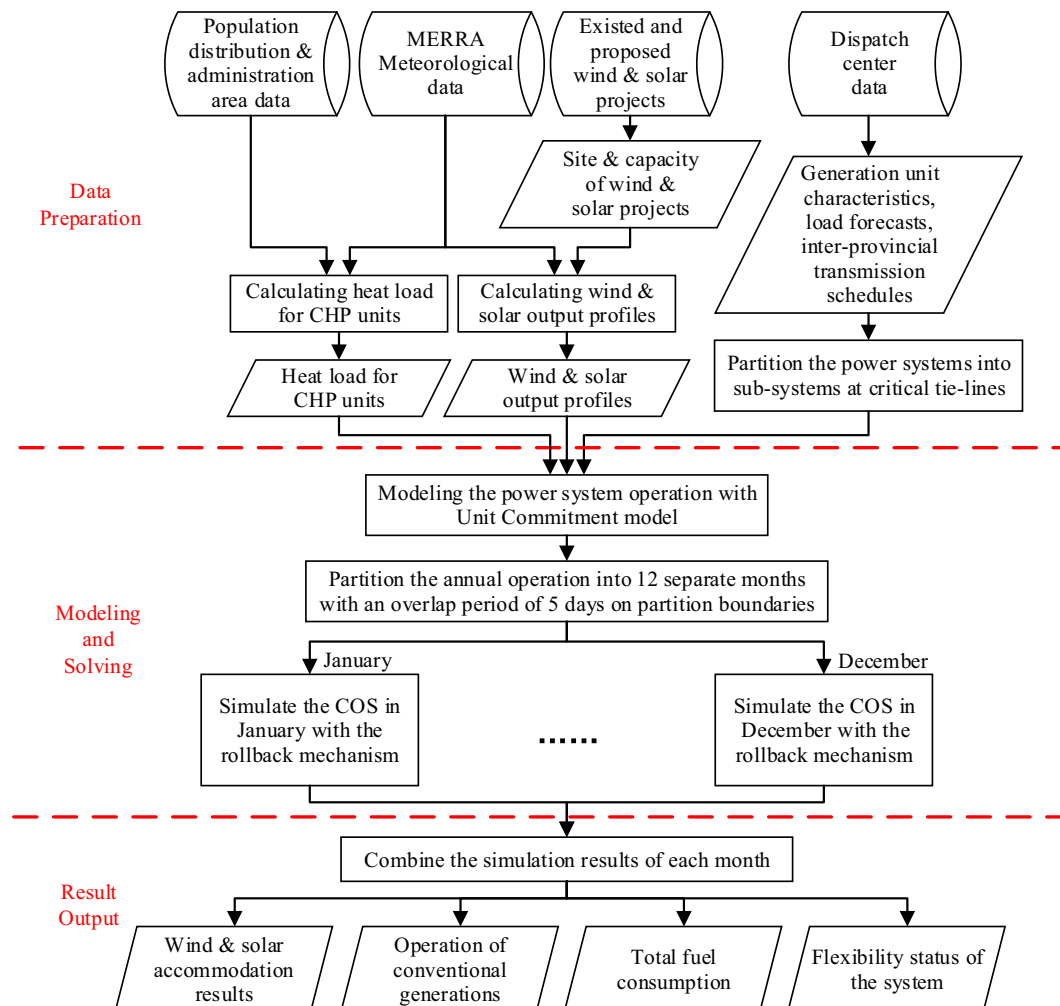


Fig. 2. Structure of the proposed simulation framework.

3. Data preparation

3.1. Converting from meteorological data to the wind and solar power output

In literature, meteorological data is frequently adopted for assessments of renewable resources [25–34]. Moreover, several researches use the meteorological data to model the hourly power output of renewable generations [35–37]. All these researches verified the feasibility of utilizing meteorological data to evaluate the resource potential and model the hourly power output of renewable energies. However, comprehensive methods of calculating the wind, solar power output and heat load for the COS with meteorological data geographic data still need further exploration.

Here we adopt the meteorological data obtained from the Modern Era Retrospective Analysis for Research and Applications (MERRA) database [38] to obtain the wind and solar power output. The MERRA provides the reanalysis of global meteorological data from 1979 to the present at an hourly temporal resolution and a $1/2^\circ$ latitude \times $2/3^\circ$ longitude spatial resolution. Within the MERRA database, the dataset of surface radiation flux and boundary layer flux provides surface solar irradiance and wind speed at 10 m and 50 m above the surface, respectively.

3.1.1. Obtaining wind power output

Most wind turbines are operating at hub heights of more than 60 m, but the MERRA only provides wind speed data at 10 m and 50 m above the surface, so the wind speed at designated hub height need to be extrapolated from 10 m and 50 m data. Assume a hub height of h_x , the wind speed at hub height can be calculated with the Least Square Power Law [25] as follow,

$$V_x = V_R \left(\frac{h_x}{h_R} \right)^{\alpha^{LS}} \quad (1)$$

where V_x denotes the wind speed at hub height, V_R is the reference wind speed at reference height h_R , α^{LS} is the LS friction coefficient, which can be calculated as

$$\alpha^{LS} = \frac{\sum_{i=1}^N \ln \left(\frac{V_i}{V_R} \right) \ln \left(\frac{h_i}{h_R} \right)}{\sum_{i=1}^N \ln \left(\frac{h_i}{h_R} \right)^2} \quad (2)$$

Here, V_i denotes the wind speed at height h_i , N is the total number of available wind speed data at heights other than h_R , since we only have 10 and 50 m data, if we take 50 m data as reference, then we have only one extra wind speed data, namely N is 1.

With the extrapolated wind speed data at the hub height, the wind power output can be calculated with the power curve of specific wind turbines, followed are the power curve of the Goldwind GW82/1500 1.5 MW wind turbine [39–40] shown in Fig. 3.

3.1.2. Obtaining solar power output

With the surface incident shortwave flux and surface temperature obtained from the MERRA surface flux database, the solar power generated from solar PV panels under maximum power point tracking (MPPT) mode at time t could be calculated with:

$$P_S(t) = C_S \cdot \frac{I_t}{1000} \cdot [1 + \gamma \cdot (T(t) - 25)] \quad (3)$$

where T_t is the surface temperature ($^\circ\text{C}$). C_S is the installed capacity of the solar farm. γ denotes the power correction factor for temperature, taking the value of $-0.005691 \text{ }^\circ\text{C}^{-1}$ for PV panels made with multi-crystal Si modules [41]. I_t denotes the incident irradiance (W/m^2) on PV panels, it can be calculated by projecting the surface incident shortwave flux I_s to the normal direction of PV panels installed with a leaning angle of β as following:

$$I_t = I_s \sin(\beta + \phi - \delta) \quad (4)$$

Here ϕ is the latitude of the PV panels installed location. The best leaning angle β for all Chinese cities can be calculated with [42] or obtained from [43], δ is the declination angle of the Sun, for the n -th day of the year, it can be calculated as [44]:

$$\delta = 23.45^\circ \cdot \cos \left(\frac{2\pi}{365} \cdot (n + 10) \right) \quad (5)$$

3.2. Obtaining heat load with meteorological data, population distribution and administration area data

District heating is widely adopted for heat supply all over the world. Among all district heating facilities, combined heat and power (CHP) generation unit is the most efficient one because it could generate heat and electricity simultaneously. However, CHP plants often operate at nearly full capacity to meet the heat demand in winter, which means they also generate electricity at nearly full capacity. Therefore, their presence not only lowers the residual load for wind, but also reduces the flexibility of the thermal generation fleet to accommodate the variable wind output. As a result, severe wind curtailment occurs at the cold winter time.

Due to the significant impact of CHP generation on renewable integrated power system operation, it is important to simulate the operation of CHP units accurately, which requires accurate chronological heat load data. Since heat demand is usually

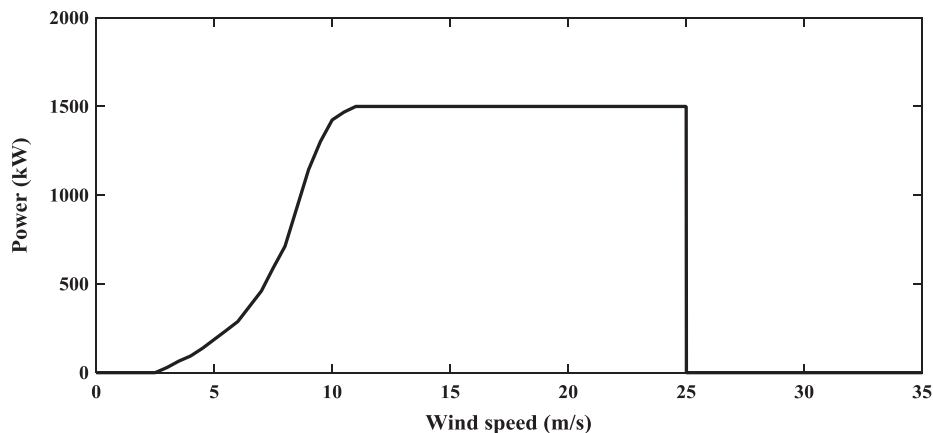


Fig. 3. The power curve of Goldwind GW81/1500 wind turbine.

balanced within each city, here we adopt the MERRA surface temperature data and population distribution data to calculate the heat load for each city.

Hourly heat load is determined by the difference between indoor and outdoor temperatures. Regional building codes require that indoor temperatures be maintained at a minimum of 18 °C [45]. The hourly ambient temperature is averaged for each city using surface skin temperature derived from MERRA grid cells, weighted by each cell's population density derived from Gridded Population of the World (GPW), v4 [46]. The administration boundary of each city is obtained from [47]. Since CHP units provide only hot water for heat supply and must be balanced within each city, the hourly heat load of the k -th city (q_k) is calculated by the following equations:

$$Q_k = \int q_k(t) \quad (6)$$

$$q_k(t) = \begin{cases} C_k \cdot \frac{18 - T_{r,k}(t)}{18 - T_{f,k}} & \text{if } T_{r,k}(t) < T_{f,k} \\ C_k & \text{elsewhere} \end{cases} \quad (7)$$

where Q_k and C_k denote total supplied hot water and heating capacity of hot water in city k , respectively, which can be derived from the China Urban Construction Statistical Yearbook [48]. $T_{r,k}(t)$ and $T_{f,k}$ represent the real ambient temperature and the full-load threshold temperature in the k -th city. Here $q_k(t)$ and $T_{f,k}$ are the variables to be solved from Eq. (6) and (7).

3.3. Partitioning the power system into sub-systems at critical tie-lines

Normally, transmission constraint of the power grids, including static and dynamic, is one of the major reasons for renewable curtailments. However, the constrained transmission lines are only a small portion of the entire power grid. In order to reduce the complexity of the COS model and accelerate the simulation speed, the power grid can be partitioned into several sub-systems at the constrained transmission lines, namely the critical tie-lines. After that, the transmission constraints within each sub-system are ignored, while the transmission constraints between different sub-systems are still kept in the model.

4. Modeling and solving

4.1. Modeling the power system operation

For a given partitioned regional power system consisting of K sub-systems, the COS framework have to provide an optimal schedule for various generation resources to satisfy both electricity and heat demands with minimum operation costs. Hence, a rigorous unit commitment model, represented as a mixed-integer linear programming (MILP), is adopted in the proposed framework to simulate the hourly operation of renewable-integrated sub-systems over a long-term horizon. To promote the renewable accommodation, penalties on the curtailments of renewables are considered. The objective consists of generators' production costs $C_i^G(t)$, start-up costs $C_i^{SU}(t)$, and shutdown costs $C_i^{SD}(t)$, as well as the penalty of curtailments on solar and wind power. The objective function is represented in Eq. (8).

$$\begin{aligned} \min F = & \sum_{k=1}^K \sum_{t=1}^H \sum_{i \in G_k} [C_i^G(t) + C_i^{SU}(t) + C_i^{SD}(t)] \\ & + \theta^S \sum_{k=1}^K \sum_{t=1}^H [\bar{p}_{S,k}(t) - p_{S,k}(t)] + \theta^W \sum_{k=1}^K \sum_{t=1}^H [\bar{p}_{W,k}(t) - p_{W,k}(t)] \end{aligned} \quad (8)$$

where G_k denotes the total number of generators in k -th sub-system, H is the total horizon of the simulation, for example, H is 8760 for a year-around simulation on the hourly basis. θ^S , θ^W are penalty coefficients for unit curtailed solar and wind power, respectively. $p_{S,k}(t)$, $p_{W,k}(t)$ are hourly consumed solar and wind power at time t in subsystem k ; $\bar{p}_{S,k}(t)$, $\bar{p}_{W,k}(t)$ are hourly available solar and wind power derived from meteorological data. The production cost ($C_i^G(t)$) is modeled as a piecewise-linear function of hourly power output of generator i to approximate the quadratic cost function [49]. The start-up and shutdown costs are modeled as linear functions of unit commitment states with the same formulation in [49].

All constraints are listed as follows.

(1) **Power balance constraint** ensures the sum of all types of generation is equal to total load power p_t^l at each time interval.

$$\sum_{i \in G_k} p_{G,i}(t) + p_{W,k}(t) + p_{S,k}(t) + T_{I,k}(t) - T_{O,k}(t) = p_{L,k}(t) \quad \forall t, k \quad (9)$$

where $p_{G,i}(t)$ is the hourly power output of generator $i \in G_k$ at time t . $T_{I,k}(t)$, $T_{O,k}(t)$ are the imported and exported power at time t through transmission lines connected to sub-system k , respectively.

(2) **Reserve requirement constraint** ensures a minimum amount of spinning reserve to keep the operation of each sub-system against unexpected contingency and forecast errors for the security.

$$\sum_{i \in G_k} [u_i(t) \bar{p}_{G,i} - p_{G,i}(t)] \geq R_k(t) \quad \forall t, k \quad (10)$$

where $u_i(t)$ denotes the binary commitment state of generator $i \in G_k$ at time t , which takes 1 if generator i is online at time t , and 0 for the offline status; and $\bar{p}_{G,i}$ denotes the maximum power output of unit $i \in G_k$ at time t . The spinning reserve requirement at time t , $R_k(t)$ can be calculated by

$$R_k(t) = r_{L,k} p_{L,k}(t) + r_{W,k} \bar{p}_{W,k}(t) + r_{S,k} \bar{p}_{S,k}(t) \quad \forall t, k \quad (11)$$

where $r_{L,k}$, $r_{W,k}$, $r_{S,k}$ are the reserve coefficients for load, wind, and solar power, respectively.

(3) **Generation range constraint** presents the physical operational limit for the power output of each online generator at each time interval.

$$u_i(t) \underline{p}_{G,i} \leq p_{G,i}(t) \leq u_i(t) \bar{p}_{G,i} \quad \forall i \quad (12)$$

where $\underline{p}_{G,i}$ is the minimum output limit of generator $i \in G_k$.

(4) **Ramping constraint** limits the change of power output from each online generator between adjacent time intervals.

$$p_{G,i}(t) - p_{G,i}(t-1) \leq r_{U,i} \bar{p}_{G,i} + N[1 - u_i(t-1)] + N[1 - u_i(t)] \quad \forall t, i \quad (13)$$

$$p_{G,i}(t-1) - p_{G,i}(t) \leq r_{D,i} \bar{p}_{G,i} + N[1 - u_i(t-1)] + N[1 - u_i(t)] \quad \forall t, i \quad (14)$$

where $r_{U,i}$, $r_{D,i}$ denote upward and downward ramping rates of generator $i \in G_k$. N is a large constant, enforcing the effectiveness of ramping limits when $u_i(t) = u_i(t-1) = 1$.

(5) **Power output constraint for start-up and shutdown events.** If generator $i \in G_k$ is going to start or shut down at time t , the power output will be constrained by (15) or (16), respectively.

$$p_{G,i}(t) \leq s_{U,i} \bar{p}_{G,i} + N u_i(t-1) \quad \forall t, i \quad (15)$$

$$p_{G,i}(t) \leq s_{D,i} \bar{p}_{G,i} + N u_i(t+1) \quad \forall t, i \quad (16)$$

where $s_{U,i}$, $s_{D,i}$ denote the maximum output ratio of start-up and shutdown events for generator $i \in G_k$.

(6) **Minimum online and offline time constraints** guarantee that each generator must be kept online or offline for at least a given time interval after it being started up or shut down.

$$\sum_{\tau=t}^{t+T_{U,i}(t)-1} u_i(\tau) \geq T_{U,i}(t)[u_i(t) - u_i(t-1)] \quad \forall t, i \quad (17)$$

$$\sum_{\tau=t}^{t+T_{D,i}(t)-1} [1 - u_i(\tau)] \geq T_{D,i}(t)[u_i(t-1) - u_i(t)] \quad \forall t, i \quad (18)$$

where $T_{U,i}(t)$, $T_{D,i}(t)$ are given as,

$$\begin{aligned} T_{U,i}(t) &= \min\{M_{U,i}, T - t + 1\} \\ T_{D,i}(t) &= \min\{M_{D,i}, T - t + 1\} \end{aligned} \quad (19)$$

$M_{U,i}$, $M_{D,i}$ are the required minimal up and down time of generator $i \in G_k$. If generator $i \in G_k$ has already been online or offline for several hours in the initial status, the online and offline time constraints for the initial condition are represented as following:

$$u_i(t) = u_{i0} \quad \forall i, t \in [1, T_{i0}]$$

$$T_{i0} = \begin{cases} M_{U,i} - U_{i0}, & \text{if } u_{i0} = 1 \\ M_{D,i} - D_{i0}, & \text{if } u_{i0} = 0 \end{cases} \quad (20)$$

where U_{i0} and D_{i0} are the initial online and offline hours for generator $i \in G_k$ respectively.

(7) **Renewable generation constraint** ensures the hourly solar and wind power output cannot exceed the available amount limited by the resources.

$$0 \leq p_{S,k}(t) \leq \bar{p}_{S,k}(t) \quad \forall t, k \quad (21)$$

$$0 \leq p_{W,k}(t) \leq \bar{p}_{W,k}(t) \quad \forall t, k \quad (22)$$

where $p_{S,k}(t) < \bar{p}_{S,k}(t)$ and $p_{W,k}(t) < \bar{p}_{W,k}(t)$ imply curtailment of solar and wind power respectively.

(8) **Inter-system transmission constraint** ensures the electric power transferred between sub-systems is limited by the transmission capacity determined by both static and dynamic stability requirements.

$$-\bar{p}_{ji}(t) \leq p_{ij}(t) \leq \bar{p}_{ij}(t) \quad \forall i, j, t \quad (23)$$

where $p_{ij}(t)$ is the power exchanged through the tie-lines connecting sub-system i with sub-system j , $\bar{p}_{ij}(t)$ and $\bar{p}_{ji}(t)$ are the available transmission capacity from sub-system i to sub-system j and from j to i considering requirements of static and dynamic stability, respectively.

(9) **Heat load balance constraint** guarantees the heat demand at each time interval in each city is supplied by CHP generators within the city.

$$\sum_{i \in \text{CHP}_m} h_i(t) = q_k(t) \quad \forall t, m \quad (24)$$

where $h_i(t)$ is the heat generated by the i -th CHP generation unit at time t , CHP_m is the set of all CHP generation units in the m -th city.

(10) **Operation range constraint for CHP generation units during the heating season** defines the feasible operation range of CHP units, which is formulated as (25) and (26). As illustrated in Fig. 4, the maximum electric power output of CHP generation unit i is constrained by both the generation capacity and the maximum steam inflow to the high-pressure cylinder. Constrained by the constant total energy input, the maximum power output decreases as the heat output increases. The lower bound of electric power output is limited by the minimum main steam inflow which is required to ensure the safety of the coal-fired boiler and the low-pressure cylinder.

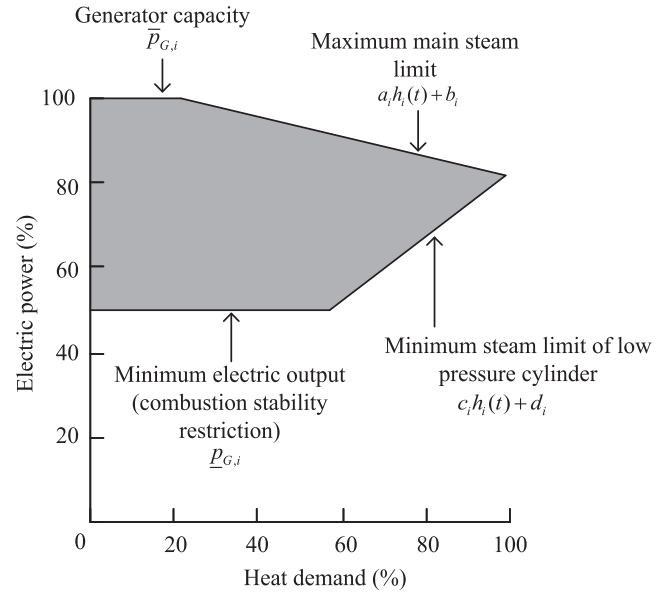


Fig. 4. Operation zone of CHP units.

$$p_{G,i}(t) \leq a_i h_i(t) + b_i \quad \forall t, i \quad (25)$$

$$p_{G,i}(t) \geq c_i h_i(t) + d_i \quad \forall t, i \quad (26)$$

4.2. Solving the simulation model with time domain partitioning and rollback mechanism

The meteorological data converting method and unit commitment model proposed above provide a feasible way to simulate power systems with high penetration renewable energy. However, due to the large number of generators in regional power systems, there could be tens of millions of variables and constraints in the model for an annual simulation, making the annual simulation hardly be solved through a single computation. Therefore, sequential simulation method is widely adopted to reduce the computational complexity for annual simulations. With the sequential simulation method, the annual simulation could be solved sequentially on a daily or weekly basis. However, when the power system has very low flexibility, namely the ramping speed is not sufficiently abundant and/or generators need too many time to start up and shut down, the initial condition of one horizon decided by the simulation of the previous horizon could lead to generators unable to follow the load. Thus, this horizon does not have feasible operation choices to safely supply the load. As a result, adopting traditional tools to carry out the year-around simulation in power systems with low flexibility could easily be infeasible at any time, and the long-term simulation will be terminated. To address the infeasible problem in the traditional sequential simulating method, this paper proposed a rollback mechanism to avoid the simulation being terminated by infeasible solution without sacrificing the computation time. The block diagram for the proposed rollback mechanism illustrates in Fig. 5. For a sequential simulation with the time interval of each n -day, the key idea of the proposed rollback mechanism consist of the following steps (m is set to 0 initially):

Step 1: set the state of last hour in day $k - m - 1$ as the initial state, simulate the operation of day $k - m$ to $k + n$;

Step 2: if the simulation of day $k - m$ to day $k + n$ is feasible, save the simulation result; if the simulation is infeasible, roll back 1 day, i.e. let $m = m + 1$ and jump to step 1;

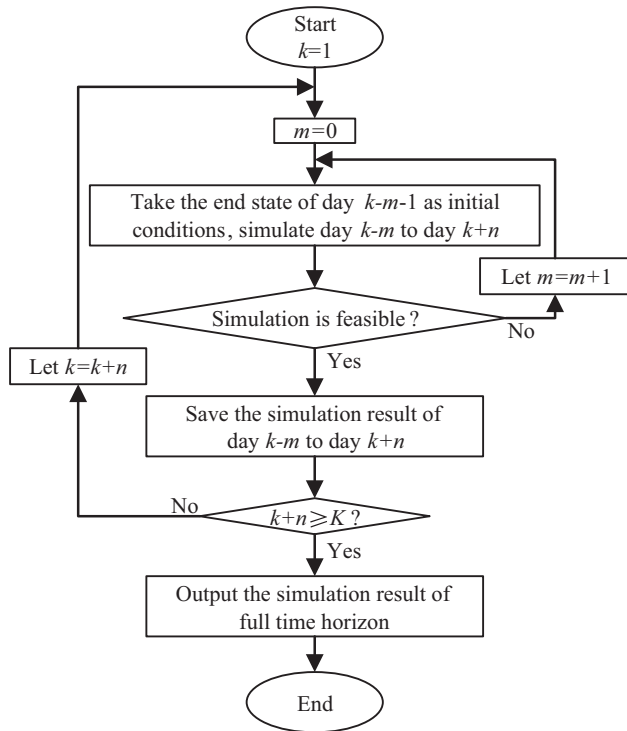


Fig. 5. Block diagram of the rollback mechanism.

Step 3: if day $k+n$ is the last day of the simulation horizon, terminate the sequential simulation and output the simulation result of the full simulation horizon; otherwise, let $k=k+n$, $m=0$ and jump to step 1;

The above-mentioned rollback mechanism could be effective in dealing with possible infeasible solutions in the year-round simulation. Due to the large amount of integer variables in the model, the year-round simulation of a large-scale power system can still take several days or even weeks to compute. To speed up the simulation, a time domain partitioning method is proposed to partition the complete simulation horizon into several sub-horizons. Thus, the sub-horizons can be solved in parallel. However, the inter-temporal connections between adjacent partitioned horizons is ignored in the simulation, which may lead to simulation results not in integrity. Since the effects of enforcement in earlier time

intervals are likely to diminish after a few days of overlap periods [50], a small overlap between adjacent sub-horizons could effectively improve the integrity of the annual result. Therefore, to trade off the computational time with the integrity of the annual simulation result, this paper divides the annual simulation horizon into 12 separate months with an overlap period of 5 days between each two adjacent sub-horizons. The adopted time domain partitioning method is demonstrated in detail in Fig. 6.

5. Case studies

5.1. Verification of the converted wind power output

The proposed wind power output converting method provides a possible way to obtain the wind power output of any wind farm with meteorological data and location of the wind farm. To verify the accuracy of the proposed wind power output data converting method, the measured wind power output data from a standard wind turbine Woniushi wind farm (located in Liaoning Province, China) is adopted to examine the output converted from meteorological data. The wind turbine installed in Woniushi wind farm is UP82-1.5 MW turbine manufactured by Unionpower, all turbines were installed at the hub height of 65 m. Here we take the wind speed from the grid cell that the wind farm located into calculated the wind speed at 65-m height, and then convert the calculated wind speed to the wind power output with the turbine's power curve. The measured and calculated wind power output from July 2 to July 15 are shown in Fig. 7. It can be seen that the calculated output well captures the major patterns of wind power, and only misses the wind power variations within 6 h. In the plotted two weeks, the measured generated wind electricity is 219.77 MWh, while the calculated electricity is 207.02 MWh, with only 5.8% relative error. Since the proposed method is aimed at simulating the long-term power system operation, usually in several months or an entire year, the wind power output converted from meteorological data should be accurate enough for long-term operations.

5.2. Verification of the converted solar power output

To verify the proposed solar power output converting method, the measured data from Changma Solar farm (located in Gansu Province, China) is adopted to compare with the output converted from meteorological data. Fig. 8 compares measured solar power output from July 2 to July 29 in 2013 with the calculated data. In the plotted three weeks, the measured solar electricity is

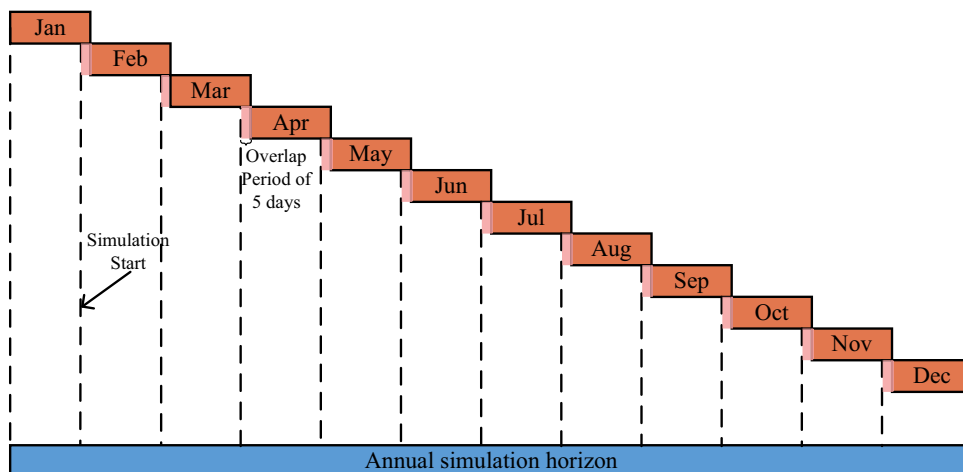


Fig. 6. Illustration of partitioning the annual simulation horizon into monthly partitions with overlap periods.

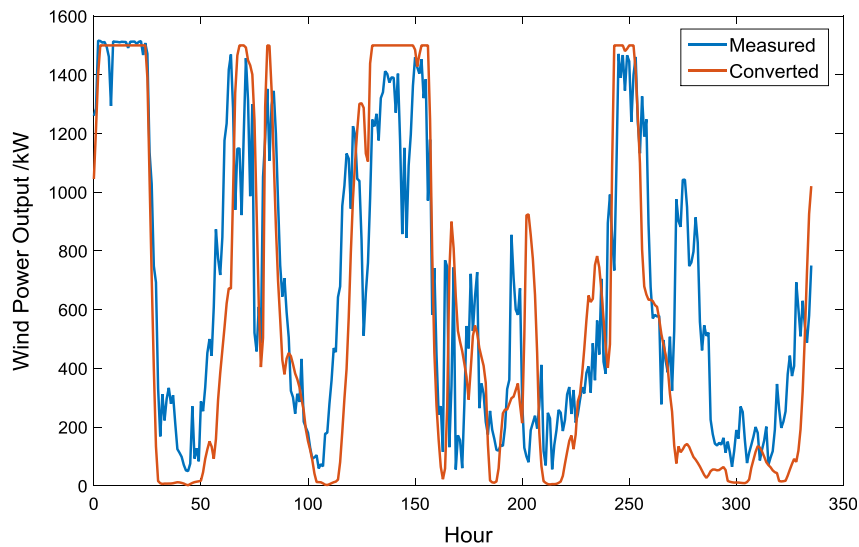


Fig. 7. Comparison of measured wind power output with the converted output.

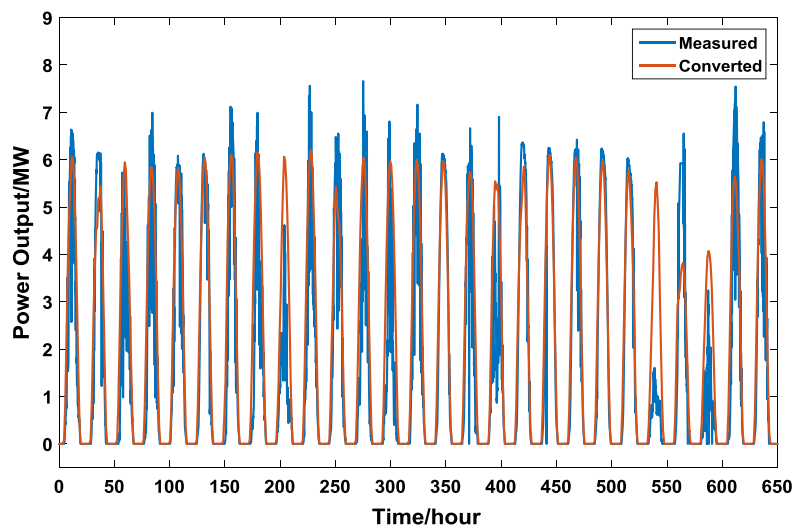


Fig. 8. Comparison of measured solar power output with the converted output.

1183.65 MW h, while the calculated electricity is 1255.8 MW h, with only 6% relative error. Similar to the conclusion in [35], the converted solar power output well captured the intra-day and inter-day patterns of practical solar power output, which verifies that converting the solar power output from meteorological data is feasible and accurate enough for the long-term operation simulation of power systems.

5.3. Analyzing the characteristics of the heat load for CHP units

China's coal-heavy power system is often regarded as the main reason of severe wind curtailments [51]. A conventional coal-fired power plant can only operate at power outputs above 50% of its rated capacity, and it takes several hours for a plant to recover from a cold start [52]. Hence, coal-fired power plants have very limited flexibility to accommodate to intrinsically variable wind power. The situation in Northern China during winter is exacerbated further by the conflicts between favorable wind and inflexible combined heat and power (CHP) generation [53].

By adopting the proposed method to calculate the heat load in Xi'an city (the capital city of Shaanxi Province) and assuming all

CHP units within the city equally share the heat load, the heat load and power output range of a typical 300 MW CHP unit between Jan 1 and Jan 14 is shown in Fig. 9. It can be found that, the heat load has a regular pattern of lower at day time and higher at night time. In addition, the variation in heat load will lead to changes in the range of electrical power output, and will lead to narrower electrical power output ranges at nights. However, the wind is most favorable in winter nights, while the flexibility of the power system is the worst in the year. As a result, severe wind curtailment occurs exactly when the potential wind output would otherwise be greatest in the year.

5.4. Verification of the simulation framework with Northwest China Grid

To demonstrate the complete process of adopting the proposed framework to simulate power system operations and to verify the accuracy of the simulation results, the Northwest China Grid (NWCG) is adopted for the case study. As shown in Fig. 10, NWCG is composed of 5 provincial grids: Shaanxi, Gansu, Qinghai, Ningxia and Xinjiang, which covers 33.1% of total land in China. The total

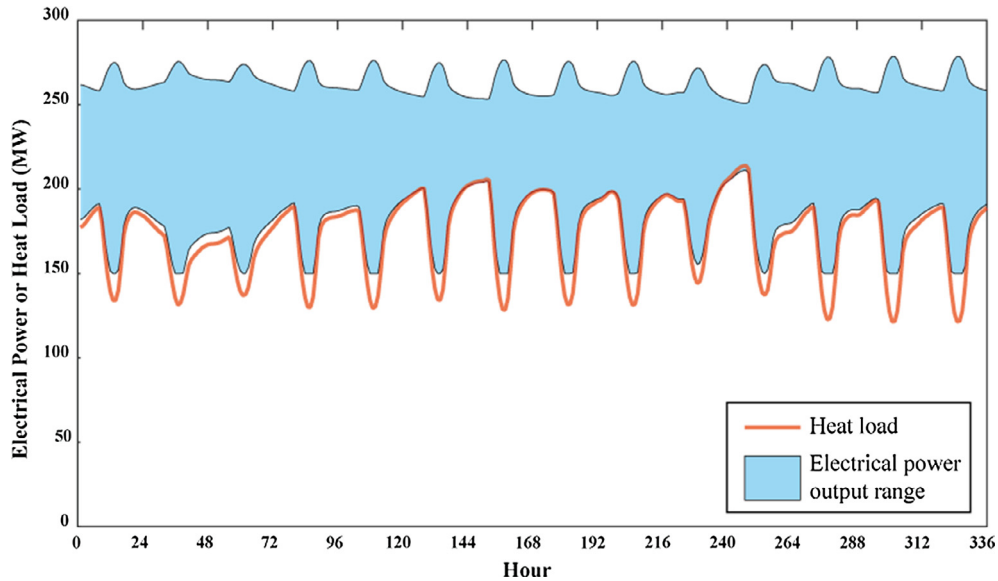


Fig. 9. Heat load and electrical power output range of a 300 MW CHP units.



Fig. 10. Northwest China Grid in 2015.

consumed electricity reached 531.4 TW h in 2015, which is almost the same as that of Germany. Meanwhile, NWCG has abundant wind and solar resources, the wind and solar capacities have reached 39.81 GW and 21.66 GW in 2015, respectively, which accounts for 30.8% and 50.2% of total wind and solar capacity in China. But behind the booming installment of wind and solar generations, nearly 32% of wind and 17.1% solar in NWCG were curtailed in 2015 because of the intensive inflexibility of the coal-heavy generation fleet.

The process of adopting the proposed framework to simulate the operation of NWCG in 2015 can be divided into the following three steps:

Step 1: Calculating wind, solar power output profiles and heat load for CHP units.

To calculate the wind and solar power output profiles, locations of the wind and solar projects are required. All the projects located within NWCG are demonstrated in Fig. 11 [54]. With the location data, we can use the meteorological and geographical data to calculate the year around wind and solar power output profiles with the proposed calculating method. Here we adopt the 2015 wind speed, solar irradiance and surface temperature data derived from MERRA, all wind farms are assumed using the same GoldWind GW82/1500 wind turbine [37]. For NWCG, the heat load is balanced within each city. Thus, we use the distribution of urban population and administration area data to calculate the heat load of each city.

Step 2: Partitioning the power system in sub-systems at the critical tie-lines.

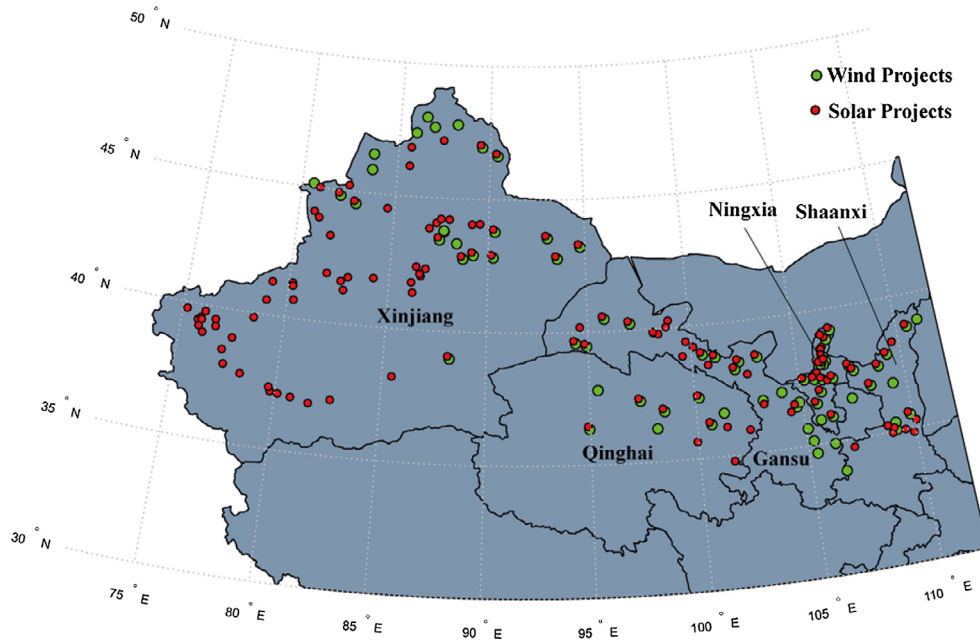


Fig. 11. Wind and solar projects in NWCG 2015.

After the rapid development of the transmission network in China in the past 20 years, the intra-provincial transmission networks is sufficiently strong now, the only bottlenecks in NWCG are the inter-provincial transmission lines. The transmission capacities of inter-provincial transmission lines are mainly constrained by dynamic stability, e.g. the N – 1 contingency, voltage stability and so on. To reduce the computation burden, the NWCG is partitioned into five provincial grids, and the transmission network within each province is ignored. The transmission capacity between the partitioned provincial grids at the beginning of 2015 are as shown in Table 1.

Table 1
Transmission capacity between partitioned provincial grids in NWCG 2015.

Sending end	Receiving end				
	Shaanxi	Gansu	Qinghai	Ningxia	Xinjiang
Shaanxi	–	4500 MW	–	–	–
Gansu	5000 MW	–	3800 MW	4100 MW	2000 MW
Qinghai	–	3800 MW	–	–	–
Ningxia	–	4100 MW	–	–	–
Xinjiang	–	2000 MW	–	–	–

Table 2
Comparison of wind and solar curtailments between simulation results and statistical data.

Data	Provinces	NEA statistics	Simulation without TDP		Simulation with TDP		Simulation using EnergyPLAN	
			Curtailment	Relative error	Curtailment	Relative error	Curtailment	Relative error
Curtailed solar (TW h)	Shaanxi	0	0	0.00%	0	0.00%	0	0.00%
	Gansu	2.87	2.81	1.93%	2.81	2.00%	0	100%
	Qinghai	0.30	0.39	31.19%	0.39	31.02%	0	100%
	Ningxia	0.25	0.25	1.15%	0.25	1.03%	0	100%
	Xinjiang	1.67	1.63	2.09%	1.64	2.00%	0	100%
	NWCG total	5.09	5.09	0.00%	5.09	0.01%	0	100%
Curtailed wind (TW h)	Shaanxi	0	0.00	0.00%	0	0.00%	0	0.00%
	Gansu	8.20	7.95	3.01%	7.96	2.95%	0.03	99.63%
	Qinghai	0	0.06	–	0.06	–	0	0.00%
	Ningxia	1.30	1.31	0.71%	1.31	0.64%	0	100%
	Xinjiang	7.10	7.00	1.45%	6.99	1.50%	0.02	99.72%
	NWCG total	16.60	16.31	1.74%	16.32	1.71%	0.06	99.64%
Computation time (second)			11775		1217		0.1	

Step 3: Adopting the proposed COS model and solving accelerating strategy to solve the annual simulation.

As indicated in Fig. 2, the calculated wind and solar power output profiles, power systems' data of all partitioned sub-systems are adopted for the simulation. The inter-provincial transmission schedules, generators' characteristics and electricity load data are obtained from the operation mode of NWCG in 2015. The proposed simulation model is implemented with YALMIP [55] in Matlab and solved with Gurobi Optimizer [56]. The comparison between simulation results and the statistical data released by NEA [22,23] and State Grid Corporation of China [24] are listed in Tables 2 and 3.

As shown in Tables 2 and 3, NWCG curtailed 16.60 TW·h of wind power and 5.09 TW·h of solar power in 2015, the simulated wind and solar power curtailments are 16.32 TW·h and 5.09 TW·h, respectively, which only have 1.69% and 0% of relative errors compared with the statistical data. And for all provinces except Qinghai, the simulated provincial wind and solar curtailments are less than 2.95% different from the practical operation results. Since both practical wind and solar curtailment are too few in Qinghai, the relative error could be very large while the

Table 3
Comparison of utilization hours between simulation results and statistical data.

Provinces	Coal-fired generation (Hour)			Hydro generation (Hour)		
	Statistic	Simulation	Relative error	Statistic	Simulation	Relative error
Shaanxi	4686	4666	0.4%	3269	3474	6.3%
Gansu	3777	4033	6.8%	4018	4002	0.4%
Qinghai	5096	4981	2.3%	3255	3346	2.8%
Ningxia	5420	5646	4.2%	3673	3854	4.9%
Xinjiang	4726	4876	3.2%	3553	3731	5.0%

absolute errors are no more than 0.09 TW h. The utilization hours of both hydro generation and coal-fired generations are shown in Table 3, it can be found that the utilization hours in the simulating results have no more than 6.8% of differences compared with the statistical data. Therefore, the simulated curtailments along with utilization hours of coal-fired generation and hydro generation are all aligned with the practical operation results, which demonstrates the accuracy of the proposed method, especially considering that the maintenance schedule of generators and intra-provincial transmission networks are ignored in the simulation.

To further illustrate the accuracy of using the proposed framework to simulate the chronological operation of power systems with low flexibility, the widely used energy system analysis tool – EnergyPLAN is adopted for a comparison [9]. The differences in operation results obtained from the proposed framework and the EnergyPLAN for the same NWCG case are also shown in Table 2. It can be found that the EnergyPLAN has significant simulation errors in the wind and solar curtailments. Since the EnergyPLAN excludes the unit commitment constraints, it severely overestimates the flexibility of the system. Therefore, it could hardly simulate the renewable energy integration in power systems with low flexibility like the NWCG accurately. That is one of the motivations to develop the proposed framework in this paper.

Besides the accuracy of the proposed simulation framework, the computation speed and reliability of the proposed framework also

outperformance conventional methods. As shown in Table 2, the computation time of simulating the 2015 operation of NWCG with the proposed framework is 20 min. Compared with requiring 196 min to compute without the proposed time-domain partitioning technique (using the same computation platform), the computation speed is increased by more than 8 times. Meanwhile, the difference in simulation result are less than 0.2%. During the annual simulation, the rollback mechanism has been triggered 5 times, which helps avoid infeasibilities in 4 months. In summary, the proposed solving acceleration strategy not only guaranteed a feasible solution but also effectively improved the computation speed.

To further verify the accuracy of the COS results, comparisons of the chronological statistics, e.g. comparison between monthly operation results and monthly simulation results, are the most reasonable choice. Due to the operation statistics are only published seasonally in China, here we adopt the seasonally accommodated electricity from wind to verify the accuracy of chronological simulation results. The statistical and simulated seasonally integrated wind electricity in each province are depicted in Fig. 12. Due to the absence of the wind generation statistics for the 3rd season in 2015, here comparisons are made for the 1st season, 2nd season and 3rd–4th season in 2015 [22,57,58]. As indicated in Fig. 12, the simulated wind integrations are in good consistency with the practical operation data, the differences between simulated results and statistical data are less than 17%.

Besides the statistical results, hourly operation results can also be obtained from the proposed framework for precise analyses. For example, the hourly power balance of February 19–24 in Xinjiang province is illustrated in Fig. 13. It can be found that the majority of wind curtailments happened at nights when the electrical load is the lowest but wind is favorable. Because of the large heat demand in winter times, CHP units must generate electricity at nearly full capacity and could hardly adjust their outputs. Therefore, the majority of electricity load is occupied by CHP generations, and the residue load is too few to accommodate all available wind

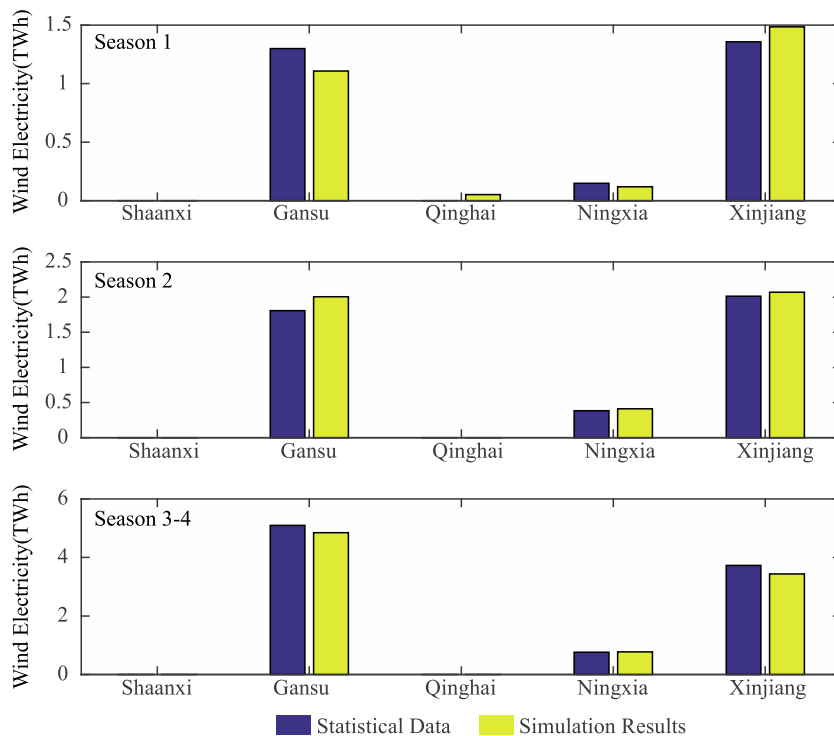


Fig. 12. Comparison of seasonally accommodated wind electricity in NWCG.

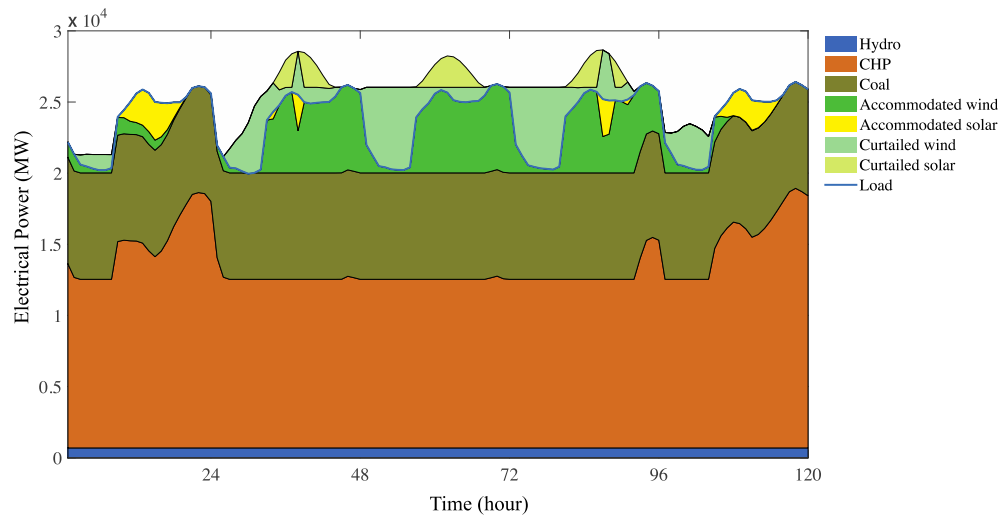


Fig. 13. Power balance in Xinjiang province.

power, as a result, the excess wind power must be curtailed. By analyzing the causes of wind curtailment in each hour in the year, it can be concluded that investing in heat storage or electrified heating facilities, the wind curtailment in Xinjiang can be reduced significantly.

The above analysis well demonstrate that the proposed COS framework could be utilized to investigate the causes of the curtailments. Since the proposed framework is a general tool capable of analyzing the integration of newly proposed renewable project or future renewable targets, it could be applied to investigate both existing curtailments and potential curtailments in the future, wherever the power system located. The curtailment analysis in Xinjiang Province also reveals that, the conflict between keeping a high level of heat supply and reducing the electrical power output for CHP units is the main causes of the wind curtailments. In fact, the renewable curtailments caused by the conflicts between CHP generation and renewable generations is a common issue all-round the globe [10,15,16,59]. Thereby, applying the proposed framework to analyze the cost-effectiveness of investments in heat pump, heat storage or heat boilers could be a general way to aid the selection of techniques to reduce the renewable curtailments all over the world.

6. Conclusion

This paper proposed the chronological simulation framework of adopting meteorological data to simulate the annual operation of regional power systems with high penetration of renewable energy. The proposed framework includes three major steps: firstly, the wind, solar power output and heat load for CHP units are converted from meteorological data; then the converted data will be inputted to the proposed COS model and solving acceleration strategy to simulate the power system operation; after that, results will be combined and outputted. The proposed method is verified with measured wind, solar output data and the official statistical operation data for NWCG in 2015. By summarizing the results of case studies, the following conclusions can be drawn,

- The wind and solar power output converted from MERRA meteorological data can well capture the major patterns of renewable power output, while some hourly scale variations are missed.
- The proposed solving acceleration strategy could increase the computation speed by more than 8 times and avoid the simulation being terminated by infeasible solutions.

- The proposed framework is demonstrated applicable to practical power systems. Adopting the proposed framework to simulate the 2015 operation of NWCG could have no more than 6.8% differences compared with the statistical data of practical operations.
- The hourly operation results obtained from the proposed framework can be used to analyze the causes of the curtailments, and help decide the most cost-effective measures to address the curtailments.

Although the cases studied in this paper all are focused in China, due to the generality of the proposed COS framework, it could also be applied to any regional power systems over the globe. Since the proposed simulation framework could generate power output profiles for the planned wind and solar projects, and can utilize the obtained renewable output data to simulate the annual operation of renewable deeply penetrated power system accurately and fast. We are currently assessing the grid-accommodation potential of solar and wind power in 2020 in China by sweeping scenarios of different renewable penetrating rates with the proposed framework. Besides that, we are also analyzing how different scheduling of the inter-provincial transmission could affect the wind and solar accommodation in China, the potential of reducing wind and solar curtailment by flexible scheduling of the inter-provincial transmission in a practical regional grid in China is going to be quantified with the proposed framework.

Acknowledgements

This research was supported by National Natural Science Foundation of China (51577075) and National Key R&D Program of China (2016YFB0900400).

We would like to thank Professor Michael B. McElroy, Mr. Chris P. Nielsen and Dr. Xinyu Chen at Harvard University for supporting this research and providing valuable feedbacks on the methodology. We also would like to thank the reviewers for their valuable comments that greatly improved the manuscript.

References

- [1] REN21. Global renewable status report 2016; 2016. <http://www.ren21.net/wp-content/uploads/2015/07/REN12-GSR2015_Onlinebook_low1.pdf>.
- [2] Yang B, Jiang L, Wang L, Yao W, Wu QH. Nonlinear maximum power point tracking control and modal analysis of DFIG based wind turbine. *Int J Electr Power Energy Syst* 2016;74:429–36.

- [3] Shen Y, Yao W, Wen JY, He HB. Adaptive wide-area power oscillation damper design for photovoltaic plant considering delay compensation. *IET Gener, Transm Distrib.* <<http://dx.doi.org/10.1049/iet-gtd.2016.2057>>.
- [4] United Nations Framework Convention Change. Report of the conference of the parties on its twenty-first session, held in Paris from 30 November to 13 December 2015; 2016. <<http://unfccc.int/resource/docs/2015/cop21/eng/10.pdf>>.
- [5] Wierzbowski M, Lyzwa W, Musial I. MILP model for long-term energy mix planning with consideration of power system reserves. *Appl Energy* 2016;169:93–111.
- [6] Connolly D, Lund H, Mathiesen BV, Leahy M. A review of computer tools for analysing the integration of renewable energy into various energy systems. *Appl Energy* 2010;87(4):1059–82.
- [7] Yu Y, Zhou J, Qin C, Wang H. Detailed operation simulation based planning alternative evaluation of power system with large-scale wind power. IEEE innovative smart grid technologies – Asia (ISGT Asia). Tianjin, China; 2012.
- [8] Hedegaard K, Münster M. Influence of individual heat pumps on wind power integration – energy system investments and operation. *Energy Convers Manage* 2013;75:673–84.
- [9] Østergaard PA. Reviewing EnergyPLAN simulations and performance indicator applications in EnergyPLAN simulations. *Appl Energy* 2015;154:921–33.
- [10] Hedegaard K. Wind power integration with heat pumps, heat storages, and electric vehicles – energy systems analysis and modelling. Roskilde: Technical University of Denmark; 2013.
- [11] Ali H, Sanjaya S, Suryadi B, Weller SR. Analysing CO2 emissions from Singapore's electricity generation sector: strategies for 2020 and beyond. *Energy* 2017;124:553–64.
- [12] Komušanac I, Čosić B, Duić N. Impact of high penetration of wind and solar PV generation on the country power system load: the case study of Croatia. *Appl Energy* 2016;184:1470–82.
- [13] Thellufsen JZ, Lund H. Roles of local and national energy systems in the integration of renewable energy. *Appl Energy* 2016;183:419–29.
- [14] Liu L, Zhu T, Pan Y, Wang H. Multiple energy complementation based on distributed energy systems – case study of Chongming county, China. *Appl Energy* 2017;192:329–36.
- [15] Bach B, Werling J, Ommen T, Münster M, Morales JM, Elmegaard B. Integration of large-scale heat pumps in the district heating systems of Greater Copenhagen. *Energy* 2016;107:321–34.
- [16] Zhang N, Lu X, McElroy MB, Nielsen CP, Chen X, Deng Y, et al. Reducing curtailment of wind electricity in China by employing electric boilers for heat and pumped hydro for energy storage. *Appl Energy* 2016;184:987–94.
- [17] Eser P, Singh A, Chokani N, Abhari RS. Effect of increased renewables generation on operation of thermal power plants. *Appl Energy* 2016;164:723–32.
- [18] Tuohy A, Meibom P, Denny E, O'Malley M. Unit commitment for systems with significant wind penetration. *IEEE Trans Power Syst* 2009;24(2):592–601.
- [19] Rong Y, Haoyong C, Gang W, Pan C. A mixed integer programming method for security-constrained unit commitment with multiple wind farms. *Automat Electr Power Syst* 2010;34(5):29–33.
- [20] Yang C, Chun L, Yuehui H, Xinsong Z, Xiaofei L, Yue Y. Wind power accommodation capability of large-scale interconnected power grid based on equivalent aggregation method. *High Voltage Eng* 2016;42(9):2792–9.
- [21] Yang C, Peng L, Yue Y, Xinsong Z, Siqi G, Chengfei Z. Analysis on accommodating capability of renewable energy and assessment on low-carbon benefits based on time sequence simulation. *Automat Electr Power Syst* 2014;38(17):60–6.
- [22] China National Energy Administration. 2015 Statistics of wind power development. <http://www.nea.gov.cn/2016-02/02/c_135066586.htm>.
- [23] China National Energy Administration. 2015 Statistics of solar power generation. <http://www.nea.gov.cn/2016-02/05/c_135076636.htm>.
- [24] State Grid Corporation. Reports on the electricity transactions in 2015:2015.
- [25] Archer CL, Jacobson MZ. Evaluation of global wind power. *J Geophys Res* 2005;110(D12).
- [26] Lu X, McElroy MB, Kiviluoma J. Global potential for wind-generated electricity. *Proc Nat Acad Sci* 2009;106(27):10933–8.
- [27] McElroy MB, Lu X, Nielsen CP, Wang Y. Potential for wind-generated electricity in China. *Science* 2009;325(5946):1378–80.
- [28] He G, Kammen DM. Where, when and how much wind is available? A provincial-scale wind resource assessment for China. *Energy Pol* 2014;74:116–22.
- [29] He G, Kammen DM. Where, when and how much solar is available? A provincial-scale solar resource assessment for China. *Renew Energy* 2016;85:74–82.
- [30] CWEAR. China wind resources assessment report. Beijing: China Meteorological Press; 2010.
- [31] Lu X, McElroy MB, Nielsen CP, Chen X, Huang J. Optimal integration of offshore wind power for a steadier, environmentally friendlier, supply of electricity in China. *Energy Pol* 2013;62:131–8.
- [32] Hong L, Moller B. Offshore wind energy potential in China: under technical, spatial and economic constraints. *Energy* 2011;36(7):4482–91.
- [33] Zhou Y, Wu W, Hu Y, Liu G. The temporal-spatial distribution and evaluation of potential solar energy resources in Northwest China. *J Nat Resour* 2010;10(25):1738–49.
- [34] Zhou Y, Wu W, Hu Y, Fang Q, Liu G. The assessment of available solar energy resources potential in Jiangsu Province. *Renew Energy Resour* 2010;28:10–3.
- [35] Richardson DB, Andrews RW. Validation of the MERRA dataset for solar PV applications. Photovoltaic specialist conference; 2014.
- [36] Richardson DB, Harvey LDD. Strategies for correlating solar PV array production with electricity demand. *Renew Energy* 2015;76:432–40.
- [37] Prasad AA, Taylor RA, Kay M. Assessment of solar and wind resource synergy in Australia. *Appl Energy* 2017;190:354–67.
- [38] Goddard Earth Sciences Data and Information Services Center GES DISC. README document for MERRA data products; 2010. <<http://disc.sci.gsfc.nasa.gov/mdisc/documentation/README.MERRA.pdf>>.
- [39] The Wind Power Database. The power curve of Goldwind GW82/1500 wind turbine. <<http://www.thewindpower.net/scripts/fpdf181/turbine.php?id=441>>.
- [40] Liu J, Wen JY, Yao W, Long Y. Solution to short-term frequency response of wind farms by using energy storage systems. *IET Renew Power Gener* 2016;10(5):669–78.
- [41] Marion B, Kroposki B, Emery K, Cueto JD, Myers D, Osterwald C. Validation of a photovoltaic module energy ratings procedure at NREL; 1999. <<http://www.nrel.gov/docs/fy99osti/26909.pdf>>.
- [42] Yunlin S, Xiaorong D, Xiaoyang W, Li L. Calculation of solar radiation and optimum tilted angle of fixed grid connected solar PV array. *Acta Energ Sol Sin* 2009;30(12):1597–601.
- [43] National Center of Supervision and Inspection on Solar Photovoltaic Product Quality (CPVT). Best leaning angles and solar generated electricity for 360 cities in China. <<http://www.cpvt.org.cn/newsdetail.aspx?id=1195>>.
- [44] Cooper PI. The absorption of radiation in solar stills. *Sol Energy* 1969;12(3):333–48.
- [45] Standard of climatic regionalization for architecture. Chinese National Standards. GB 50178-93; 1994.
- [46] Center for International Earth Science Information Network (CIESIN), Columbia University. Documentation for gridded population of the world, Version 4 (GPWv4); 2016. <<http://sedac.ciesin.columbia.edu/binaries/web/sedac/collections/gpw-v4/gpw-v4-documentation.pdf>>.
- [47] GADM database of Global Administrative Areas. <<http://gadm.org/>>.
- [48] Ministry of Housing and Urban-Rural Development of the People's Republic of China. China Urban Construction Statistical Yearbook: China Statistics Press; 2014.
- [49] Carrion M, Arroyo JM. A computationally efficient mixed-integer linear formulation for the thermal unit commitment problem. *IEEE Trans Power Syst* 2006;21(3):1371–8.
- [50] Barrows C, Hummon M, Jones W, Hale E. Time domain partitioning of electricity production cost simulations; 2014. <http://www.researchgate.net/publication/302987790_Time_Domain_Partitioning_of_Electricity_Production_Cost_Simulations>.
- [51] Davidson MR, Zhang D, Xiong W, Zhang X, Karplus VJ. Modelling the potential for wind energy integration on China's coal-heavy electricity grid. *Nat Energy* 2016;1(7):16086.
- [52] Kang C, Chen X, Xu Q, Ren D, Huang Y, Xia Q, et al. Balance of power: toward a more environmentally friendly, efficient, and effective integration of energy systems in China. *IEEE Power Energ Mag* 2013;11(5):56–64.
- [53] Lu X, McElroy MB, Peng W, Liu S, Nielsen CP, Wang H. Challenges faced by China compared with the US in developing wind power. *Nat Energy* 2016;1(6):16061.
- [54] China Renewable Energy Engineering Institute. Renewable energy database. <<http://red.renewable.org.cn:9080/RED/search.action?index=2&db=2&order=Col=dt>>.
- [55] Löfberg J. YALMIP: a toolbox for modeling and optimization in MATLAB. CACSD conference. Taipei, Taiwan; 2004.
- [56] Gurobi GmbH. Gurobi Optimizer. <<http://www.gurobi.com/products/gurobi-optimizer>>.
- [57] China National Energy Administration. Statistics on wind power integration in the first season of 2015. <http://www.nea.gov.cn/2015-04/28/c_134190553.htm>.
- [58] China National Energy Administration. Statistics on wind power integration in first half of 2015. <http://www.nea.gov.cn/2015-07/27/c_134451678.htm>.
- [59] Li J, Fang J, Zeng Q, Chen Z. Optimal operation of the integrated electrical and heating systems to accommodate the intermittent renewable sources. *Appl Energy* 2016;167:244–54.